

08,16

Study of an ideal hybrid perovskite — gold interface by the stationary Green's operator method

© N.I. Alekseev^{1,2}, A.N. Aleshin¹, I.V. Oreshko^{1,2}

¹ Ioffe Institute,
St. Petersburg, Russia

² St. Petersburg State Electrotechnical University „LETI“,
St. Petersburg, Russia

E-mail: NIAlekseyev@yandex.ru

Received February 8, 2025

Revised February 9, 2025

Accepted February 10, 2025

The study examines the hybrid interface between MAPbX₃ type halide perovskite and gold — one of the electrode materials that are considered as the best possible. The interface is recognized as an ideal one that forms a superlattice, which is partly implemented in the known literature. Investigation carried out by the stationary Green's operator method shows that gold levels above the Fermi energy form surface states, to which metal electrons can move (metal-induced states), in the perovskite band gap. Together with the intense electromigration of halogen ions in hybrid perovskites, such movement provides an effective current transport channel in perovskite cells.

Keywords: hybrid perovskites, metalorganic perovskites, organic-inorganic interface, Green's operator method.

DOI: 10.61011/PSS.2025.02.60681.28-25

1. Introduction

Hybrid perovskite (HP) crystals — (MA)PbX₃ structures, where X is halogen, MA is the CH₃NH₃ molecules, combine promising properties that are inherent in perovskites in general and significant for the development of memristive memory devices, solar cells SC and other optoelectronic devices [1–3]: high solar radiation absorption coefficient inside thin films; weak bond in an exciton, which is important for separation of electrons and holes during radiation absorption; long charge carrier diffusion allowing the carriers to move within SC, and others.

Compared with inorganic perovskite, hybrid perovskite features low densities of „common“ carriers — electrons and holes — at level (10⁹–10¹³) cm⁻³ and low energies of lattice damage (and intense halogen ion electromigration).

HP technology progress is associated both with the development of process techniques and deeper understanding of processes taking place at and near the perovskite-rectifying electrode interface.

Besides the electromigration of perovskite components within perovskite, surface states (SS) arising at the interface are substantial for such processes. Evaluation of the SS role is well illustrated by the title of review [4]: Halide Perovskites: is it all about the Interfaces? Recent work [5] provides a full review of the current investigation level in the field of SS.

This work is devoted to semianalytic modelling of SS. Together with the electromigration analysis that was partially addressed in [6], such model makes it possible to interpret the temperature dependence of the current-voltage curve of a memristive structure and provides an approach to more complex tasks, in particular, to resistive switching. These tasks will be addressed in a separate work.

Gold was chosen as a material for an electrode that forms the interface with perovskite. This is due to the fact that gold is not an electrochemically active material, transfer of which between electrodes could form conductive wires (such method to control the on-off state of a memristive gap is currently considered as the least promising).

However, chemical stability of gold interacting with the halide component of HP is currently in doubt. There is also information that a gold atom, when exposed to light, can substitute a heavy atom in perovskite forming a system with alternating elongated and flattened tetragons and doubled lattice constant [7].

A layer of such material, partly hypothetical, shall form an additional interlayer between gold and HP. However, as it follows from our estimates, in terms of the lattice constant it matches well with both gold and perovskite and doesn't introduce qualitative changes into the study.

Though, a low-defect interface between gold and HP lattices requires a high technology level, it was probably successfully implemented in [8,9]. Therefore, it will be methodologically correct to assume that such connection is implemented. Actually, if a cubic lattice constant $a_{\text{HP}} = 6.28 \text{ \AA}$ is taken for the CH₃NH₃PbI₃ hybrid perovskite lattice, and a tabular value $a_{\text{gold}} = 4.704 \text{ \AA}$ (in the (100) planes) is taken for a FCC gold lattice, then a superlattice with a very small and, therefore, real compliance constant $a_{\text{Compl}} = 18.744 \text{ \AA}$ is permissible, which corresponds to 3.9848 (four) of the gold cell and 2.9848 (three) of the perovskite cell. Then a relative lattice mismatch for gold is 0.038. Mismatch energy per matching lattice cell area $A_0^2 = 351.56 \text{ \AA}^2 = 3.52 \text{ nm}^2$ is approx $2.55 \cdot 10^{-3} \text{ eV}$, i.e. is very low. Thus, the selection of the pair of material at the interface may be considered as reasonable.

2. Employed calculation and evaluation method

Some kind of quantum-chemical (QC) application program package could be an optimum way to determine the density of states $\text{DOS}(E)$ — in this case of surface or interface states $\text{DOSS}(E)$, if a larger superstructure constant along the interface and an equally large nominal constant across the interface could be set in this package. But in real practice, even the former constant is too large, and a simplified semianalytic solution has to be used. It is based on the stationary Green's operator technique (SGOT) in — stationary Green's operator technique) in site representation described in the works by S.Yu. Davydov [10–13].

The solution uses one of the simplest options — tight-binding approximation and interactions of only the nearest neighbors. However, several more substantial electron orbitals assigned to a particular type of atoms are considered in this case. SGOT for a periodic lattice is based on the Dyson equation in the operator

$$\hat{G} = \hat{g} + \hat{g}\hat{V}\hat{G} \quad (1)$$

or expanded matrix forms

$$G_{ik} = g_{ik} + g_{il}V_{lm}G_{mk} \quad (2)$$

(where m, k are indices of particular sites). This equation is a form of the Schrödinger equation representation $(E - \hat{H})\hat{G} = \hat{I}$, where the Hamiltonian \hat{H} is $\hat{H} = \hat{H}_0 + \hat{V}$, and unperturbed Hamiltonian \hat{H}_0 satisfies the equation $(E - \hat{H}_0)\hat{g} = \hat{I}$. Equation (1) is solved together with the translation-invariant TI conditions. According to common rules, zero in the denominator of elements G_{ik} found in course of solution defined a dispersion equation of electronic band structure.

At the first calculation step, it may be considered that \hat{g} corresponds to a system of isolated lattice atoms that don't interact with each other; each atom contains an electron energy level or a group of levels. In case of one level, the matrix of g_{ik} elements of the operator \hat{g} : $g_{ik} = \delta_{ik}(E - \varepsilon_0)^{-1}$ contains only one diagonal element g_{00} .

A solution obtained by SGOT contains only atomic level energies and orbital overlap integrals V_{ik} at one or neighboring atoms as necessary parameters. In the HP–gold system, ε, V (playing, in fact, a role of adjustable parameters) for each of the materials may be obtained by combining the QC and DFT calculation data of infinite 3D materials, perovskite and gold, with the SGOT scheme. These calculations in this work were performed in Quantum Espresso.

Then, the perovskite and gold energy level overlap integrals restored from these packages and data calculated by other authors are used to calculate Green's operator elements \hat{G} and dispersion relations for the HP–gold interface. A necessary step at this calculation stage involves obtaining \hat{G} operator for „bare“ perovskite and gold interfaces, with respect to which bond cutting plays a role of perturbation. To avoid confusion, another notation of \hat{G} is used — \hat{Q} with

corresponding indices, for HP–gold finite interface — $\hat{\Pi}$ is used.

To implement the DOSS evaluation program, a system of rules was formulated to account for the band width and position of band centers considering the interaction between this energy level and at least several nearest levels and at least for the simplest lattices. These rules may be referred to as a set of primitives.

The simplest primitive is a simple cubic lattice with the constant a , only one s electron with ε_0 at each atom and a single overlap integral $V < 0$. The Dyson equation together with the TI conditions gives the diagonal element expression of \hat{G}

$$G_{00} = g_{00} \left(1 - 2g_{00}V(\cos(k_x a) + \cos(k_y a) + \cos(k_z a)) \right)^{-1}, \quad (3)$$

pole of which gives the known dispersive relation

$$\varepsilon_k = \varepsilon_0 + 2V(\cos(k_x a) + \cos(k_y a) + \cos(k_z a)), \quad V < 0 \quad (4)$$

for a single band. A unique property of a simple cubic lattice is that the dispersive relation maintains the form of (4) (without $\cos(k_z a)$) for a semi-space, i.e. there is an interface mode. The same refers to FCC.

The next in complexity is a simple cubic lattice, neighboring atoms of which interact through the s -electron on one atom and p -electron on a neighboring atom („simple salt“ with alternating simple metal and halogen atoms Halide Perovskites: is it all about the Interfaces?). In this case, the scheme of solutions of the system of Dyson equations taking TI into account gives G_{00} written as [10]:

$$G_{00} = \frac{g_{00}}{1 - 4g_{00}Vg_{11}V \sin^2 ka} = \frac{E - \varepsilon_1}{(E - \varepsilon^+)(E - \varepsilon^-)} = \frac{1}{\varepsilon^+ - \varepsilon^-} \left(\frac{\varepsilon^+ - \varepsilon_1}{E - \varepsilon^+} + \frac{\varepsilon_1 - \varepsilon^-}{E - \varepsilon^-} \right), \quad (5)$$

where $\varepsilon^+(\mathbf{k})$ and $\varepsilon^-(\mathbf{k})$ are dispersive dependences of the upper (antibonding) and lower (bonding) bands located above ε_1 and below ε_0 , respectively:

$$\varepsilon^{(\pm)} = \frac{\varepsilon_1 + \varepsilon_0}{2} \pm \left(\left(\frac{\varepsilon_1 - \varepsilon_0}{2} \right)^2 + 4V^2 \left(\sin(k_x a) + \sin(k_y a) + \sin(k_z a) \right)^2 \right)^{1/2}. \quad (6)$$

When deriving (5–6), it was assumed that an electron with ε_0 („ s “ electron) was bound to atom „0“ an electron with $\varepsilon_1 > \varepsilon_0$ was located on atom 1 (and atoms translationally equivalent to it).

For simplicity, (6) is written for the 1D lattice. The 3D case differs only in the square of sum of three, rather than one, sines in the denominator. Each of the $\varepsilon^\pm(\mathbf{k})$ bands has the following width

$$\left(\left(\frac{\varepsilon_1 - \varepsilon_0}{2} \right)^2 + 12V^2 \right)^{1/2} - \left(\frac{\varepsilon_1 - \varepsilon_0}{2} \right). \quad (7)$$

According to a common calculation scheme of the local density of states on atoms with electrons $\varepsilon_0, \varepsilon_1$, $\text{DOS}_{0(3D)}$, $\text{DOS}_{1(3D)}$, all states satisfying the dispersion law $\varepsilon(\mathbf{k})$ are summed over \mathbf{k} ; in this case, it is convenient to introduce an infinitely small imaginary additive to the denominator of \hat{G} elements. In particular,

$$\text{DOS}_{0(3D)}(E) = \frac{2(2a)^3}{(2\pi)^3} \int_{\text{BZ}} \frac{1}{\pi} \text{Im} G_{00}(\mathbf{k}) d\mathbf{k}, \quad (8)$$

where with a sufficiently general form of G_{00} :

$$G_{00} = \frac{A(E)}{K(E) - K(\varepsilon_{\mathbf{k}}) - i0} \quad (9)$$

DOS is proportional to

$$\begin{aligned} \text{DOS}_{0(3D)}(E) &\sim \int_{\text{BZ}} A(E) \delta(K(E) - K(\varepsilon_{\mathbf{k}})) d\mathbf{k} \\ &= \int \left(A(E) \frac{dK}{dE} \frac{dE}{d\mathbf{k}_x} \right)_{E=\varepsilon_{\mathbf{k}}}^{-1} d\mathbf{k}_y d\mathbf{k}_z, \quad (10) \end{aligned}$$

the proportional factor can be conveniently written in each particular case. For G_{00} written as (9) and a simple cubic lattice with the constant $2a$

$$\begin{aligned} \text{DOS}_{0(3D)}(E) &= \frac{2a^3}{\pi^3} \\ &\times \int_{-\pi/2a}^{\pi/2a} \frac{((\varepsilon^+ - \varepsilon_1)\delta(E - \varepsilon^+) + (\varepsilon_1 - \varepsilon^-)\delta(E - \varepsilon^-))}{\varepsilon^+ - \varepsilon^-} d^3\mathbf{k} \quad (11) \end{aligned}$$

and for the upper energy band with $\varepsilon^+(k)$, we get:

$$\begin{aligned} \text{DOS}_{0(3D)}(E > \varepsilon_1) &= \frac{2a^2}{\pi^3} \int_{-\pi/2a}^{\pi/2a} \left(\frac{d\varepsilon_{\mathbf{k}}}{dk_x} \right)^{-1} d\mathbf{k}_{\perp} \\ &= \frac{2a^2}{\pi^3} \int_{-\pi/2a}^{\pi/2a} d\mathbf{k}_{\perp} \frac{\varepsilon^+ - \varepsilon_1}{\varepsilon^+ - \varepsilon^-} \left(\frac{dQ}{dk_x} \right)_{k_x=k_x(E, \mathbf{k}_{\perp})}^{-1}, \quad (12) \end{aligned}$$

where

$$\begin{aligned} Q &= \sqrt{\left(\frac{\varepsilon_1 - \varepsilon_0}{2} \right)^2 + 4V^2(3 - 2(C_x + C_y + C_z))}; \\ C_{x,y,z} &= \cos(2k_{x,y,z}a). \end{aligned}$$

Then, in the form convenient for elementary numerical counting

$$\begin{aligned} \text{DOS}_{0(3D)}(E > \varepsilon_1) &= \frac{2(E - \varepsilon_1)}{\pi^3 V^2} \\ &\times \int_{-\pi/2}^{\pi/2} [1 - (3 - C_y - C_x - 2t)]^{-1/2} dq_y dq_z \quad (13) \end{aligned}$$

— function of the single parameter

$$t = \left(((E - \langle \varepsilon \rangle)/2V)^2 - (\Delta\varepsilon/4V)^2 \right).$$

„Simple salt“ equations are convenient when the real interaction structure is complicated and the dispersion equation has a high order in E . Moreover, these equations provide a vivid picture of level expansion to bands and shift of the centers of any pair from initial levels as a result of mutual „rapping“ of levels on the energy scale.

Dependence of the density of states of the upper antibonding band (i.e. a band with $E > \varepsilon_1$) is given in Figure 1 with $(\varepsilon_1 - \varepsilon_0)/4|V| = 1$, the density of states with $E < \varepsilon_0$ is in mirror position on the other side of the band gap with $\varepsilon_1 - \varepsilon_0$, i.e. to the left of curves 1, 2, 3 in the orientation as shown in Figure 1.

Note that the density of states in the band formed by its „own“ energy level (for example, $\text{DOS}_1^{(\varepsilon_1)}$) changes near the band edges according to the root law (boundaries of curve 1 in Figure 1); density of states formed by another level changes according to the square law (left boundary of curve 2). With the energy of the density of states corresponding exactly to a particular level that are formed by the interaction with higher and lower levels, it is reduced (in Figure 1, this is illustrated by a dashed line to the left of point $(E - \langle \varepsilon \rangle)/2|V| = 1$, i.e. $\varepsilon = \varepsilon_0$ — by a band formed by some reference level higher than ε_1 and not taken into consideration).

3. Dispersive relations and density of states of infinite HP perovskite and gold

When proceeding to 3D lattices of HP and gold, we make qualitative remarks derived from the calculation of electron structure of these materials in [14–17].

Perovskite valence band (VB) is formed by orbitals $5s$ of iodine (I), $5p$ of iodine, and $6s$ of lead (Pb), CB is formed by orbitals $6p$ (Pb). MA cations are „far away from the scene“ — below band $5s$, and don't contribute to the bands adjoining the Fermi energy. Level $6s$ of I in this case includes a whole set of sublevels that generates a set of overlapping bands [14]. Local densities of states on Pb and I atoms calculated in [15] are shown in Figure 2 with minor simplifications; all sublevels $6s$ are considered as a single level.

Note that the complication of equations (11)–(13), that occurs when interactions $6s-5p$, $6p-5s$, $5p-6p$ between orbitals of neighboring atoms and $5p-5s$, $6p-6s$ on an individual atom are taken into account, is purely formal, if perovskite is still considered in the „simple salt“ model. We give the resulting equations without deduction. Initial matrix of coefficients in the system of Dyson equations for Green's operator elements G_{11}^{6p6p} , G_{11}^{6z6p} , G_{01}^{5z6p} , G_{01}^{5p6z} , G_{01}^{5p6p}

is written as

$$\begin{pmatrix} 1 & -g_1^{6p}V_{11}^{6s6p} & -g_1^{6p}(-2iSE+V_{10}^{6p5s}) & -g_1^{6p}2CE+V_{10}^{6p5p} & \\ -g_1^{6s}V_{11}^{6s6p} & 1 & 0 & -g_1^{6s}(-2iSE+V_{10}^{6s5p}) & 0 \\ -g_0^{5s}2iSE-V_{01}^{5s6p} & 0 & 1 & -g_0^{5s}V_{00}^{5s5p} & 0 \\ -g_0^{5p}2CE-V_{01}^{5p6p} & -g_0^{5p}2iSE-V_{01}^{5p6s} & -g_0^{5p}V_{00}^{5p5s} & 1 & 0 \\ -g_0^{5p}2iSE-V_{01}^{5p6p} & 0 & 0 & 0 & 1 \end{pmatrix} \quad (14)$$

where $S = \sin(ka)$, $C = \cos(ka)$, $E^\pm = \exp(\pm ika)$. Matrix (14) is written for a one-dimensional problem. For the 3D case, it is sufficient to replace $S^2 \rightarrow (S_x + S_y + S_z)^2$.

Then for G_{00}^{6p6p} of Green's operator, we obtain

$$G_{11}^{6p6p} = \frac{(A - BS^2)}{[K - DS^2 + (R - FS^2)^2]}, \quad (15)$$

where the Pb atom with atomic orbitals 6s, 6p is designated as „0“, the I atom with orbitals 5p, 5s is designated as „1“, $S^2 = (S_x + S_y + S_z)^2$,

$$\begin{aligned} \xi_0^{5s} &= E - \varepsilon_{5s}, & \xi_0^{5p} &= E - \varepsilon_{5p}; \\ \xi_1^{6s} &= E - \varepsilon_{6s}, & \xi_1^{6p} &= E - \varepsilon_{6p} \end{aligned} \quad (16)$$

— shifts of E with respect to the considered levels. Notations A, B, K, D are similar to those introduced in (9), — polynomials with respect to ξ

$$A(E) = \xi_0^{5s} \xi_0^{5p} \xi_1^{6s} - \xi_1^{6s} (V_{00}^{5s5p})^2, \quad B(E) = 4\xi_0^{5s} (V_{10}^{6s5p}),$$

$$\begin{aligned} K(E) &= \xi_1^{6p} \xi_1^{6s} \xi_0^{5s} \xi_0^{5p} - \xi_1^{6s} \xi_1^{6p} (V_{00}^{5p5s})^2 \\ &\quad - \xi_0^{5s} \xi_0^{5p} (V_{11}^{6s6p})^2 - 4\xi_1^{6p} \xi_0^{5s} (V_{10}^{6p5p})^2, \end{aligned}$$

$$D(E) = 4 \left[\xi_0^{5s} \xi_1^{6p} (V_{10}^{6s5p})^2 + \xi_0^{5p} \xi_1^{6s} (V_{10}^{6p5s})^2 - \xi_0^{5s} \xi_1^{6s} (V_{10}^{6p5p})^2 \right],$$

$$R = V_{11}^{6s6p} V_{00}^{5s5p}, \quad F = 4V_{10}^{6s5p} V_{10}^{6p5s}. \quad (17)$$

The local density of states 6p on the Pb atom is given, as in (9)–(11), by a double integral that is easily taken numerically:

$$\begin{aligned} \text{DOS}_{1(\text{Pb})}^{6p} &= \frac{16a^2}{\pi^3} \int_0^{\pi/2a} dk_y dk_z \left(\frac{(A - BS^2)}{2S_x C_x} \right. \\ &\quad \times \left. \frac{\frac{dK}{dE} + 2R \frac{dR}{dE} - S^2 \frac{d}{dE} (D + FR) + 2F \frac{dF}{dE} (S^2)^2}{D + 2FR - 2F^2 S^2} \right)_{E=\varepsilon_k} \end{aligned} \quad (18)$$

where

$$S^2 = \frac{(D + 2RF) \pm \sqrt{D^2 + 4F(DR - FK)}}{2F^2} \quad (19)$$

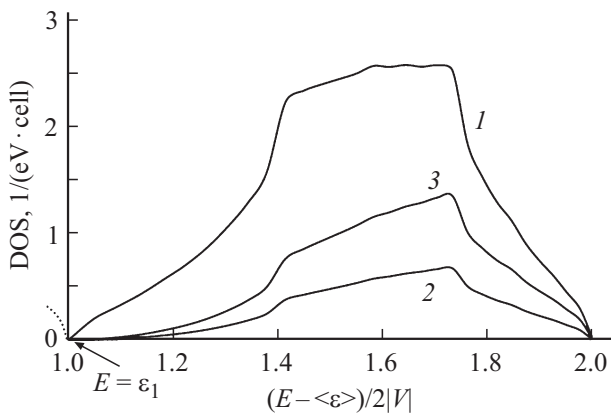


Figure 1. Densities of states of the upper (antibonding) band $E > \varepsilon_1$ that are responsible for initial electron orbitals $\varepsilon_{0,1}$ with $(\varepsilon_1 - \varepsilon_0)/4|V| = 1$. 1 and 2 — DOS_1 and DOS_0 with $V = 1 \text{ eV}$, 3 — DOS_0 with $V = 0.5 \text{ eV}$.

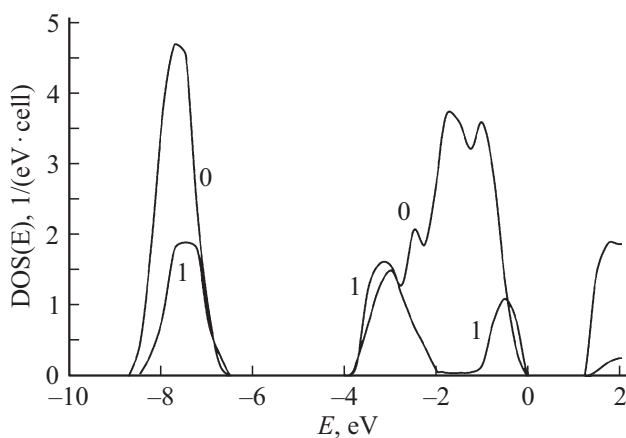


Figure 2. Simplified picture of the local densities of states (LDOS) calculated in [14] for MA perovskite PbI_3 . „0“ — LDOS on iodine atoms, „1“ — LDOS on lead atoms. Zero energy — LDOS of VBM perovskite (DOS_{Pb} , adopted Pb diagram file).

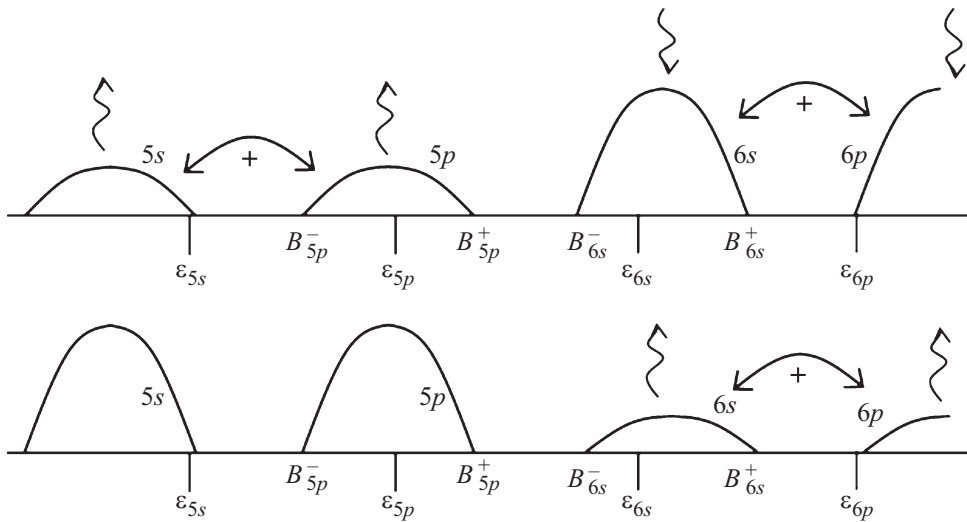


Figure 3. Illustrative relations of local densities of states calculated on the Pb atom (upper figure) and halogen atom (lower figure) in the simple two-band scheme approximation (equations (11)–(13)) (taken from the Band Scheme file, page 6).

— biquadratic equation solution in the denominator (15),

$$S_x = \sqrt{\frac{(D + 2RF) \pm \sqrt{D^2 + 4F(DR - FK)}}{2F^2}} - S_y - S_z;$$

$$C_x = \sqrt{1 - S_x^2}. \quad (20)$$

Other densities of states also have a similar form.

When the specifics of perovskite lattice (more complicated than that of the „simple salt“ type) is not taken into account for levels 5s, 5p, 6s, 6p and the form of DOS curve is known (Figure 2), five overlap integrals V_{5p6s} , V_{5s6p} , V_{5s5p} , V_{6p6s} , V_{5p6p} may be defined from (15)–(20) and five local density ratios $\text{DOS}_0^{(5s)}/\text{DOS}_0^{(5p)}$, $\text{DOS}_0^{(5s)}/\text{DOS}_0^{(6s)}$, etc., that are given in Figure 2. The problem is not exactly correct, because there are seven such ratios, as can be seen in Figure 2.

Overlap integrals were determined numerically. The total squared error of the determination of the ratio of densities of states was minimized by one of integrals V_{5p6s} , V_{5s6p} , V_{5s5p} , V_{6p6s} , V_{5p6p} at a time. Then, another integral was varied, etc. Thus, the procedure had a gradient descent character in dimensionality 5 space and converged quite slowly, however, three of five desired overlap integrals V_{5p6s} , V_{5s5p} , V_{6p6s} ultimately were little different from the initial values that may be easily obtained from elementary equations of type (7).

These values of V are obtained from the known perovskite bandwidths (Figure 2), providing that each width in any direction on the energy scale is determined by the interaction with only the nearest levels. Given $B_{5p}^-, B_{5p}^+ \approx B_{6s}^-, B_{6s}^+$ are the boundaries of bands 5p and 6s. The upper boundary of band 5s and lower boundary of band 6p coincide with energies of these states ε_{5s} and ε_{6p} , because bands 5s and 6p have neighbors only on one side

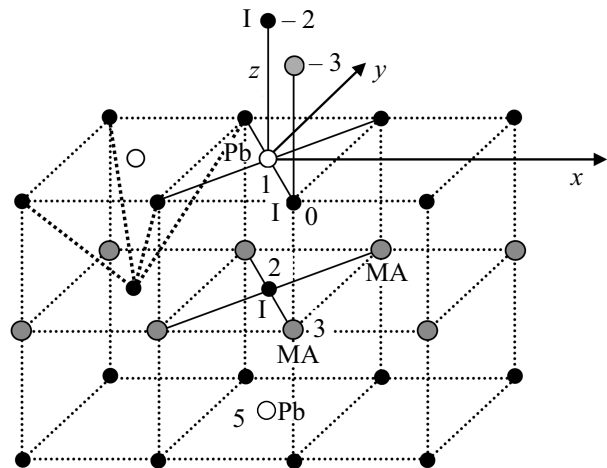


Figure 4. Designations of atoms in the perovskite lattice cell. White circles — Pb atoms, black circles — halogen atoms (atoms 0,2), gray circles — MA atoms. Halogen tetrahedron edges are shown in the left upper corner.

of the energy scale. Then the „upper“ FWHM of band 6s is

$$B_{6s}^+ - \varepsilon_{6s} = \left(\left(\frac{\varepsilon_{6s} - \varepsilon_{5p}}{2} \right)^2 + 12(V_{6s5p})^2 \right)^{1/2} - \frac{\varepsilon_{6s} - \varepsilon_{5p}}{2}$$

whence it follows that the integral

$$V_{6s5p} = -\frac{\sqrt{3}}{6} \left[(B_{6s}^+ - \varepsilon_{6s})(B_{6s}^+ - \varepsilon_{5p}) \right]^{1/2}. \quad (21)$$

Symmetrically, the following expression may be written immediately for the same quantity

$$V_{6s5p} = -\frac{\sqrt{3}}{6} \left[(\varepsilon_{6s} - B_{5p}^-)(\varepsilon_{6p} - B_{6s}^-) \right]^{1/2},$$

to correct the position of levels $6s$ and $5p$ (typical dips on DOS on curve „0“ in Figure 2 indicate the initial position of these levels). In two other integrals

$$V^{6s6p} = +\frac{\sqrt{3}}{6} \left[(\varepsilon_{6s} - B_{6s}^-)(B_{6s}^+ - \varepsilon_{5p}) \right]^{1/2},$$

$$V^{5s5p} = +\frac{\sqrt{3}}{6} \left[(B_{6s}^- - \varepsilon_{5p})(B_{6s}^- - \varepsilon_{5s}) \right]^{1/2} \quad (22)$$

plus sign corresponding to rapping of s and p orbitals on each of the Pb and I atoms was chosen. The sign is selected due to the fact that DOS on the I atoms is much higher than on the Pb atoms (Figure 2). On the other hand, within the simplest model (11)–(13), DOS_I that refer to the Pb atoms shall be much higher than DOS_I from the I atoms (on top of Figure 3) and vice versa. Fitting of the rapping overlap integrals removes this anomaly as is schematically shown by wavy arrows in Figure 3.

Outcomes of evaluation using equations (21)–(22) updated during a further iteration procedure are as follows: $V_{5p6s} = -0.55$ eV, $V_{6p6s} = 0.51$ eV, $V_{5s5p} = 1.0$ eV. Two other integrals obtained during such procedure: $V_{5s6p} = -0.71$ eV, $V_{6p6s} = 0.4$ eV.

We further consider that the perovskite lattice cell is more complicated than the simple salt cell. The (MA)PbX₃ lattice consists of cubic lattices of singly charged MA and Pb cations inserted one inside the other and a tetrahedral lattice of halogen ions with the centers of tetrahedra on the Pb ions (Figure 4). Thus, Pb is in the center of a tetrahedron, rather than of a cube. We assume initially that each of the atoms is connected only to the nearest neighbors, moreover, at the next but one electron orbital on each of the atoms (Figure 4).

It follows from the comparison of this picture with Figure 2 that $6s(\text{Pb})$ and $5p(\text{I})$, which are the nearest in energy, shall be taken as such minimum set of orbitals. The calculated band structure may be referred as the third primitive.

Given atom „1“ in Figure 4 is the Pb atom (as before) adjacent to the I atoms; all elements of \hat{G} that refer to the I atoms are associated with atom „0 through TI ratios. A horizontal plane above atoms 0 and 1 in Figure 4 is considered as a future plane of rupture of the perovskite crystal (the (001) plane). With such approach the matrix of the coefficients of the system of equations for the calculation of \hat{G} elements of the infinite crystal G_{11} , G_{01} , G_{21} , G_{31} is written as:

$$\begin{pmatrix} 1 & -g_1 V_{10} M & -g_1 V_{12} \eta_z^- & 0 \\ -g_0 V_{10} M^* & 1 & 0 & -g_0 V_{03} \eta_z^- \\ -g_2 V_{12} \eta_z^+ & 0 & 1 & -g_2 V_{23} M \\ 0 & -g_3 V_{03} \eta_z^+ & -g_3 V_{23} M^* & 1 \end{pmatrix}, \quad (23)$$

where V_{10} , V_{12} , V_{03} , V_{23} are overlap integrals known from Figure 4. Column on the right side of the system includes element g_1 — seed element $g_{11} = (E - \varepsilon_1)^{-1}$, other seed elements are written as $g_0 \equiv g_{00} = g_2 = g_{22} = (E - \varepsilon_0)^{-1}$.

Complex factors e_z^\pm , η_z^\pm , MM^* are determined as follows

$$e_z^\pm = \exp(\pm 2ik_z a_z); \quad \eta_z^\pm = 1 - e_z^\pm;$$

$$e_{x,y}^\pm = \exp(\pm ik_{x,y} a_x), \quad MM^* = 4 \sin^2 \frac{k_x a_x}{2} \sin^2 \frac{k_y a_x}{2}. \quad (24)$$

Solution of system (23) is given by

$$G_{11} = g_1 (1 - g_2 g_3 V_{23}^2 MM^* - g_0 g_3 V_{03}^2 \eta_z^- \eta_z^+) / D_{3D}^{(\text{HP})} \quad (25)$$

where the matrix determinant for 3D problem $D_{3D}^{(\text{HP})}$ is equal to

$$D_{3D}^{(\text{HP})} = 1 - g_2 g_3 V_{23}^2 MM^* - g_0 g_3 V_{03}^2 \eta_z^+ \eta_z^-$$

$$+ g_1 V_{10} MM^* (-g_0 V_{10}^* (1 - g_2 g_3 V_{23}^2 MM^*)$$

$$- g_0 g_2 g_3 V_{03} V_{12} V_{23} \eta_z^+ \eta_z^-)$$

$$- g_1 V_{12} \eta_z^+ \eta_z^- (g_0 g_2 g_3 V_{10} V_{03} V_{23} MM^*$$

$$+ g_2 V_{12} (1 - g_0 g_3 V_{03}^2 \eta_z^+ \eta_z^-)). \quad (26)$$

Taking into account that the interaction with MA for the Fermi energy neighborhood in an accurately calculated DOS is inessential, we discard the summands with V_{03} , V_{23} and write \hat{G} elements, that are interesting for further solution, in the same approximation:

$$D_{3D}^{(\text{HP})} = 1 - g_1 g_2 V_{10}^2 MM^* - g_2 g_1 V_{12}^2 \eta_z^+ \eta_z^-,$$

$$D_{3D}^{(\text{HP})} G_{01} = g_1 g_0 M^* \{ V_{10} (1 - g_2 g_3 V_{23}^2 MM^*)$$

$$+ g_2 g_3 V_{12} V_{23} V_{03} \eta_z^+ \eta_z^- \} \approx g_1 g_0 M^* V_{10},$$

$$D_{3D}^{(\text{HP})} G_{21} = g_2 g_1 \eta_z^+ \{ V_{12} + g_0 g_3 V_{03} (V_{10} V_{23} MM^*$$

$$- V_{12} V_{03} \eta_z^+ \eta_z^-) \} \approx g_2 g_1 \eta_z^+ V_{02},$$

$$D_{3D}^{(\text{HP})} G_{31} = g_3 g_1 \eta_z^+ M^* \{ g_0 V_{10} V_{03} + g_2 V_{12} V_{23} \} \approx 0,$$

$$G_{11} \approx g_1 / D_{3D}^{(\text{HP})}. \quad (27)$$

Determinant (26) is virtually identical to that in the „simple salt“ type simple cubic lattice with pairwise $s-p$ interaction of electron orbitals, therefore the study may use a simulated expression of such lattice and previously obtained overlap integrals.

Former calculations of the band structure of the second component of the emerging interface — gold — [16,17] show that the conduction band corresponds to closely spaced d-states. Energy level of the s-state is located deeply in VB, and s-electrons are not involved in the electron transport. The picture of the density of states of the infinite FCC lattice of gold calculated in Quantum Espresso is shown in Figure 5 without refinement of bands.

The curve in Figure 5 is interesting by the abundance of narrow energy bands above the Fermi energy („zero“ point). During formation of a stable superlattice of such metal and semiconductor, these bands can form metal

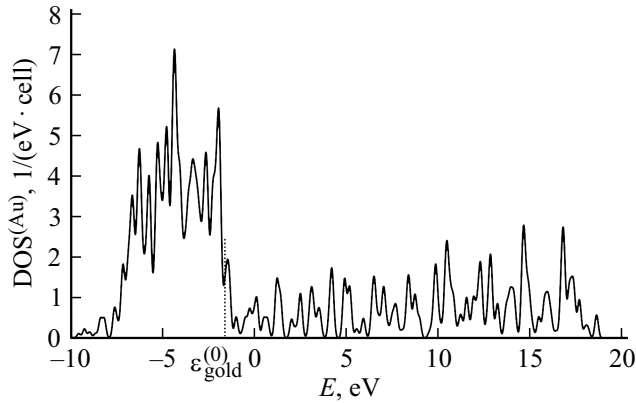


Figure 5. Density of states of gold near the Fermi energy calculated in Quantum Espresso. Zero corresponds to the Fermi energy ε_F (-5.1 eV with respect to vacuum).

induced gap states (MIGS) in the upper band gap, that are associated with the penetration of the wave function tails of superfermionic electrons into the semiconductor [8,18,19].

Figure 5 also shows that a large amount of electron orbitals associated with d-levels interact in gold. However, to get illustrative dispersive relations, we initially use an expression for the central matrix element of $\hat{Q}^{(\text{gold})}$ in a system with only one s-level:

$$Q_{00}^{(\text{gold},3D)} = \frac{g_0^{(\text{gold})}}{1 - 4V_{gg}g_0^{(\text{gold})}(C_x C_y + C_x C_z + C_y C_z)}, \quad (28)$$

where $C_{x,y,z} = \cos(k_{x,y,z}a_{\text{gold}}/2)$.

„0“ in (28) and several following equations (29)–(31) is not associated with iodine and means only some gold lattice site selected as a central one. The overlap integral V_{gg} corresponds to interacting electrons on neighboring atoms. If, as it is the case for gold, d-electrons in the xy , yz , xz planes are dominating, due to the type of symmetry of their orbitals, cosines in (28) change to sines:

$$Q_{00}^{(\text{gold},3D)} = \frac{g_0^{(\text{gold})}}{1 - 4V_{dd}g_0^{(\text{gold})}(\Sigma_x \Sigma_y + \Sigma_x \Sigma_z + \Sigma_y \Sigma_z)}, \quad (29)$$

where $\Sigma_{x,y,z} = \sin(k_{x,y,z}a_{\text{gold}}/2)$; notation V_{dd} is introduced for the overlap integral.

To consider the interaction of this d-orbital with other d-orbitals, we write the system of Dyson equations for the central element

$$G_{00}^{\text{dd}} = g_0^{(d)} + t g_0^{(d)} (V_{dd} G_{00}^{\text{dd}} + V_{d_1 d_1} G_{00}^{d_1 d_1} + V_{d_2 d_2} G_{00}^{d_2 d_2})$$

in a simple 3-level system accounting for the interaction between d-orbital and two orbitals with the nearest energy; t is the translational factor that takes into account the type of orbital and lattice symmetry. Determinant of the system of equations for G_{00}^{dd} , $G_{00}^{d_1 d_1}$, $G_{00}^{d_2 d_2}$ is written as

$$\begin{pmatrix} 1 & t g_0^{(d)} V_{dd} & -t g_0^{(d)} V_{d_1 d_1} & -t g_0^{(d)} V_{d_2 d_2} \\ -t g_0^{(d_1)} V_{d_1 d} & 1 & -t g_0^{(d_1)} V_{d_1 d_1} & -g_0^{(d_1)} V_{d_1 d_2} \\ -t g_0^{(d_1)} V_{d_2 d} & -t g_0^{(d_1)} V_{d_2 d_1} & 1 & -t g_0^{(d_1)} V_{d_2 d_2} \end{pmatrix}$$

with the right-side column consisting of a single non-zero element $g_0^{(d)}$. Some elements of the complex t shall be replaced with t^* , but the details of products and powers of t are easier to be restored in the final result. Then the numerator in the expression for G_{00}^{dd} is equal to

$$g_0^{(d)} \left(1 - |t| g_0^{(d_1)} V_{d_1 d_1} - |t| g_0^{(d_2)} V_{d_2 d_1} + t t^* g_0^{(d_1)} g_0^{(d_1)} (V_{d_1 d_1} V_{d_2 d_2} - (V_{d_1 d_2})^2) \right),$$

and the determinant can be conveniently written for $V_{d_1 d_1} = V_{d_2 d_2} = V_{dd}$, $V_{d_1 d_2} = V_{d_1 d} = V_{d_2 d} = V$:

$$\begin{aligned} & 1 - |t| V_{dd} (g_0^{(d)} + g_0^{(d_1)} + g_0^{(d_2)} + \dots) \\ & + t t^* (V_{dd}^2 - V^2) (g_0^{(d)} g_0^{(d_1)} + g_0^{(d_1)} g_0^{(d_2)} + g_0^{(d_1)} g_0^{(d_2)}) \\ & - |t| t^* g_0^{(d)} g_0^{(d_1)} g_0^{(d_2)} (V_{dd} - V)^2 (V_{dd} + 2V) \\ & + t^4 g_0^{(d)} g_0^{(d_1)} g_0^{(d_2)} (V_{dd} - V)^2 (V_{dd}^2 - V^2). \end{aligned} \quad (30)$$

When an attempt is made to consider other states of d-electrons (d_3 , d_4 , etc.) even with constant V and V_{dd} , that don't depend on the „d“ number, all terms of the sum beginning from the third term increase sharply as the number of states grows. Being unaware of the V_{dd} , $V_{d_1 d_2}$ behavior depending on the state indices and seeking only a qualitative result, we assume $|V_{dd}| = |V|$. In this case, all terms of the sum, beginning from the third one, fall out, and the internal summation in the second term with „d“ — $(g_0^{(d)} + g_0^{(d_1)} + g_0^{(d_2)} + \dots)$, may be approximately replaced with the integral, considering that all d-levels are evenly distributed over the energy scale in $\Delta\varepsilon$ steps (certainly, when $E > \varepsilon_{\text{gold}}^{(0)}$ and $E < \varepsilon_{\text{gold}}^{(0)}$, $\Delta\varepsilon$ is different). Then, when estimating the total density of states as the integral of $\text{Im}(Q_{00}^{(\text{gold},3D)} + Q_{11}^{(\text{gold},3D)} + \dots)/\pi$ over \mathbf{k} , where

$$\begin{aligned} Q_{mm}^{(\text{gold},3D)} &= g_m^{(\text{gold})} \left[1 - 4V_{dd} (\Sigma_x \Sigma_y + \Sigma_x \Sigma_z + \Sigma_y \Sigma_z) \right. \\ &\times \left. (g_0^{(\text{gold},d)} + g_0^{(\text{gold},d_1)} + \dots + g_m^{(\text{gold},d_m)} + \dots) - i0 \right]^{-1}, \end{aligned} \quad (31)$$

only $g_0^{(\text{gold},d_m)}$ contributes to each term „m“ therefore, the calculation is in no way different from the summation of simpler expressions (28)–(29) with „0“ replaced with the current „m“. Density of states at each d-level with number m calculated later depending on $\theta = (E - \varepsilon_m)/4V_{dd}$ in the definition domain $\text{DOS } \theta \in [-1, 3]$ may be approximated by

$$\begin{aligned} \text{DOS}_{m,(\text{dold},3D)} &= D_{\text{max}} \exp\left(-((\theta - 1)/\Delta)^2\right) \\ &\times \sqrt{(3 - \theta)(1 + \theta)} \end{aligned} \quad (32)$$

with the dimensionless width of the density of states $\Delta \approx 0.5$. Comparing (32) with the real DOS in Figure 5 and

requiring the minimality of the mean deviation of FWHM, peak amplitudes and „background“ component of DOS from actual values, we obtain $V_{dd} \approx 2.0$ eV, $\Delta\varepsilon \approx 0.8$ eV. Changes made to $Q_{mm}^{(\text{gold})}$ elements in transition from the bulk material to the „bare“ two-dimensional interface are minimum and will be discussed below.

4. Dispersive relations and density of states in the semi-infinite perovskite problem

In case of cutting of the vertical bonds of atoms 1 and -2 , 0 and 3 (included in the cutting lattice cell in Figure 4), a system of 4 Dyson equations occurs in the simplest model of one $6s-5p$ interaction for a new set of four elements Q_{11} , Q_{-21} , Q_{01} , Q_{-31} of \hat{Q} (index „1“ $\leftrightarrow 6s(\text{Pb})$, $0 \leftrightarrow 5p(\text{I})$). Taking into account that bond cutting across the z axis doesn't change the translational relations in the (xy) plane, the order of system is reduced to three. Then, in the first order in $V_{03} \ll V_{12}$ (i.e. weakness of interaction between halogen and MA), we get the following solution

$$D_{2D}^{(\text{HP})} Q_{11} = G_{11} - \bar{V}_{03} \left(G_{11} (G_{03} e_z^+ - G_{30} e_z^-) - (G_{13} G_{01} e_z^+ + G_{10} G_{31} e_z^-) \right),$$

$$D_{2D}^{(\text{HP})} Q_{-21} = D_{-21} - \bar{V}_{03} G_{22} \bar{V}_{21} (G_{01} G_{13} e_z^+ + G_{31} G_{10} e_z^-),$$

$$D_{2D}^{(\text{HP})} Q_{01} = (1 - G_{12} e_z^+ \bar{V}_{21}) [G_{00} \bar{V}_{03} G_{31} e_z^- + G_{01}],$$

$$D_{2D}^{(\text{HP})} Q_{-31} = (1 - G_{12} e_z^+ \bar{V}_{21}) (G_{31} e_z^- + G_{33} G_{01} \bar{V}_{03}). \quad (33)$$

Overlap integrals with bars above them in (33) — are the same as the integrals without bar, but with the „minus“ sign, because the meaning of perturbation is in zeroing the vertical bonds, determinant

$$D_{-21} = \begin{vmatrix} G_{21} e_z^- & -G_{22} \bar{V}_{20} \\ G_{11} & 1 - G_{12} e_z^+ \bar{V}_{21} \end{vmatrix} \\ = G_{21} e_z^- + \bar{V} (G_{11} G_{22} - G_{12} G_{21}),$$

and the whole determinant $D_{2D}^{(\text{HP})}$ of the „bare“ interface of perovskite is

$$D_{2D}^{(\text{HP})} = (d_{3D}^{(\text{HP})})^{-2} \xi_0 \left[d_{3D}^{(\text{HP})} (\xi_0 \xi_1 - V_{10}^2 MM^*) + \xi_0 \bar{V}_{21}^2 [V_{21}^2 \eta_z^- \eta_z^+ - \xi_0 \xi_1] \right], \quad (34)$$

where

$$d_{3D}^{(\text{HP})} = \xi_0 (\xi_0 \xi_1 - V_{10}^2 MM^* - V_{12}^2 \eta_z^- \eta_z^+), \quad \xi_{0,1,2} = (E - \varepsilon_{0,1,2}) \quad (35)$$

— nominator of 3D-determinant $D_{3D}^{(\text{HP})}$, that doesn't contain $(E - \varepsilon)^{-1}$ type poles and is convenient for the numeric solution:

$$D_{3D}^{(\text{HP})} = \frac{\xi_1 \xi_0 - V_{10}^2 MM^* - V_{12}^2 \eta_z^- \eta_z^+}{\xi_1 \xi_0}. \quad (36)$$

Finally in this approximation

$$Q_{00} = \frac{\xi_1}{(\xi_0 \xi_1 - V^2)}, \quad Q_{-21} = \frac{V(1 + \eta_z^+ e_z^-)}{(\xi_0 \xi_1 - V^2)}. \quad (37)$$

V_{10} and V_{12} in (37) are assumed equal to each other and to V . MM^* type terms with periodicity along the z axis, which is impossible for cutting across this axis, are also discarded. As it will be seen at the next solution step, such periodic terms are quite difficult to be implemented across the interface. Thus, the elements of \hat{Q} don't have any band structure at all, even along the interface, which is somewhat unexpected. Result (37) can be easily generalized to the case of several overlap integrals and $6s$, $6p$, $5s$, $5p$ levels of the perovskite components. In particular,

$$G_{11}^{6p6p} = \frac{\xi_0^{5s} \xi_0^{5p} \xi_1^{6s} - \xi_1^{6s} (V_{00}^{5s5p})^2 - \xi_0^{5s} (V_{10}^{6s5p})^2}{\xi_0^{5p} \xi_0^{5s} \xi_1^{6s} \xi_1^{6p} - \xi_1^{6s} \xi_1^{6p} (V_{00}^{5p5s})^2 - (V_{10}^{6p5s})^2 \xi_0^{5p} \xi_1^{6s} - (V_{10}^{6s5p})^2 \xi_0^{5s} \xi_1^{6p} + (V_{10}^{6s5p} V_{10}^{6p5s})^2}. \quad (38)$$

Other components of G_{00} , G_{11} are written by a symmetry argument.

5. Green's operator of the density of states at the HP — gold interface

„Side“ view and „top“ views of the HP — gold interface are shown in Figure 6 (atoms in Figure 6, B are not signed, but have the same color as in Figure 6, A).

As it was mentioned in the Introduction, gold atoms overlap every 4-th iodine atom (I) and every 4-th Pb atom in the interface superlattice. Since it is difficult to calculate such superlattice accurately, details of the most substantial overlap integrals of Au–HP are required. We proceeded from the bond energies provided (by the order of magnitude) by the heat of reactions of formation of gold iodide and dilead–gold type compounds. The first reaction of simple Au, I₂ substances releases heat of about 60 kJ/mol per two AuI „molecules“ in the lattice, with each of them having 8 bonds with the nearest atoms, i.e. 4 bonds per a molecule. The bond energy in AuI may be then assumed equal to $U_{\text{AuI}} = -0.1$ eV. Binding of gold with lead is much more difficult and comes with heat input of about 6 kJ/mol. Hence, it is possible to evaluate the energy of Au–Pb bond and, consequently, the overlap integral $U_{\text{AuPb}} = +0.015$ eV. This value is very low, therefore, it is reasonable to represent the Au–Pb interaction as a weak averaged repulsion of atoms that do not overlap in the superlattice. With such approach, there is no sense in separating $6s$, $6p$, $5s$ or $5p$ -electrons, it is sufficient to reduce them to one $6s(\text{Pb})$ electron and $5p(\text{I})$, (as it is considered in (36)–(37)).

If the Au–Pb interaction is neglected (leaving only Au–I in the match sites), the system of Dyson equations for the elements of new Green's operator $\hat{\Pi}$ reads maximally simple:

$$\Pi_{00} = Q_{00} + Q_{00} U \Pi_{00} + Q_{0a} U \Pi_{00}, \\ \Pi_{a0} = Q_{a0} + Q_{a0} U \Pi_{a0} + Q_{aa} U \Pi_{00}.$$

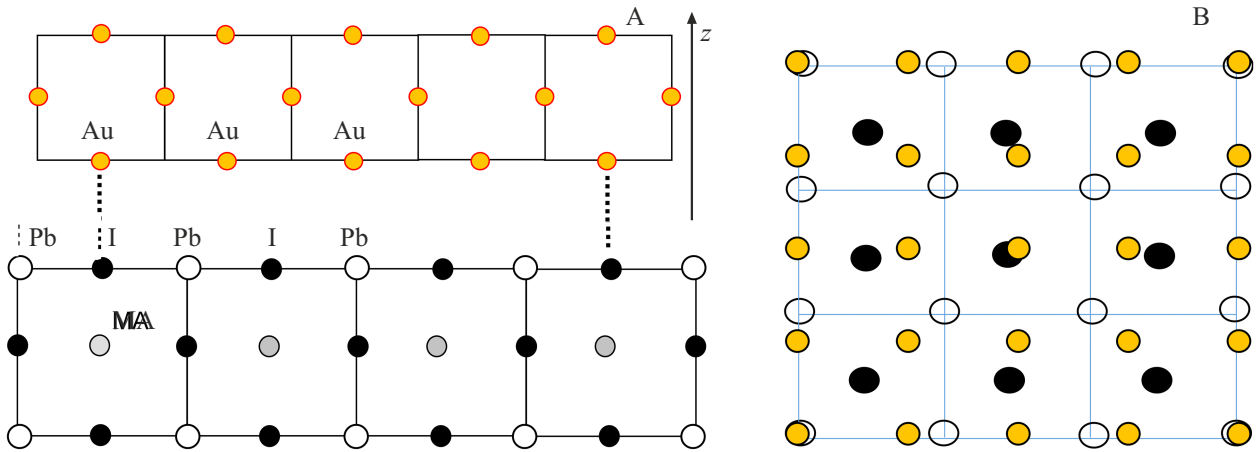


Figure 6. „Side“ view ((100) plane (A) and „top“ (B) view of the HP — gold interface.

Here, U is the overlap integral between the overlapping nodal gold and iodine atoms, indices „0“ refer to iodine, indices „a“ refer to gold. The determinant of this system is determined as

$$1 - U(Q_{0a} + Q_{a0}) + U^2(Q_{0a}Q_{a0} - Q_{00}Q_{aa}).$$

However, we cannot limit ourselves to such approach, because the states above the perovskite valence band ceiling are of utmost interest (VBM — VB maximum), but they belong to 6s level, i.e. exactly to Pb.

It can be shown that the consideration of weaker overlap integrals between the perovskite and gold interface atoms that are located outside the lattice overlap sites and are shown in Figure 7 adds one summand, that is equal in the first order in $U' \ll U$ to $-U'(Q_{0a} + Q_{a0}) + 2UU'(Q_{0a}Q_{a0} - Q_{00}Q_{aa})$, to the determinant per a reference pair of weak Au–Pb, Au–I bonds. U' was hereinafter taken equal to the arithmetic mean between one halves of U_{AuI} and U_{AuPb} , i.e. — 0.3 eV.

If a simulated 1D interface (Figure 7) is assumed to have 6 Au–Pb overlap integrals (Figure 7), then the number of weak bonds in a 2D cutting lattice cell is approx 36, i.e. 18 pairs, and the whole dispersive relation takes the form of

$$1 - U_1(Q_{0a} + Q_{a0}) - UU_2(Q_{00}Q_{aa} - Q_{0a}Q_{a0}) = 0, \quad (39)$$

where

$$U_1 = U + 18U'; \quad U_2 = U + 36U'.$$

It can be seen that the addition of interaction U' written quite approximately is of fundamental importance due to a large number of bonds.

When solving (39), the form of \hat{Q} elements for the „bare“ gold interface, including many levels and bands, shall be preferable simplified. First, for 2D \hat{Q} — in (31)

$$Q_{00}^{(gold,2D)} = g_0^{(gold,m)} \left(1 - 4V_{dd}\Sigma_x\Sigma_y \times (g_0^{(gold,0)} + g_0^{(gold,1)} + \dots + g_0^{(gold,m)} + \dots) - i0 \right)^{-1}$$

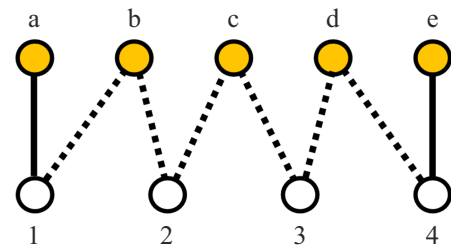


Figure 7. Scheme of averaged weak binding between the perovskite (numbers) and gold (letters) interface atoms.

periodic summand $\Sigma_x\Sigma_y$ will be maintained. In $L = g_0^{(gold)} + g_1^{(gold)} + \dots + g_m^{(gold)} + \dots$ it is convenient hereinafter to extract numbers of m and $m + 1$ bands between energies of which E is embedded, and to replace the sum of other functions $g_0^{(gold,i)}$ approximately with integral, so

$$L = (E - \epsilon_m)^{-1} + (E - \epsilon_{m+1})^{-1} + \int_{m+1}^{n_{max}^{(1)}} \frac{dm'}{E - \Sigma_x\Sigma_y V_{dd} - (\epsilon_{gold}^{(0)} + m'\Delta\epsilon)} + \int_1^{m-1} \frac{dm'}{E - \Sigma_x\Sigma_y V_{dd} - (\epsilon_{gold}^{(0)} + m'\Delta\epsilon)} + \int_0^{n_{max}^{(1)}} \frac{dm'}{E - \Sigma_x\Sigma_y V_{dd} - (\epsilon_{gold}^{(0)} - m'\Delta\epsilon)}. \quad (40)$$

The output of expression L in (40) reduces to the sum of logarithms (hence its notation) and depends on the position of point E on the energy axis. If level $\epsilon_{gold}^{(0)}$ is in coincidence with the point of sharp decrease in DOS in Figure 5 and $E > \epsilon_{gold}^{(0)}$, the first integral in L (upward

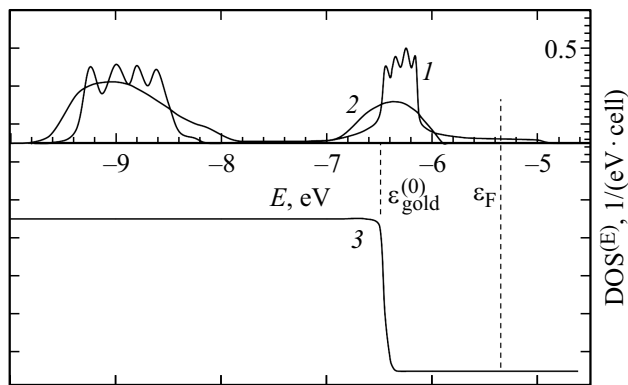


Figure 8. Total density of states at the perovskite-gold interface. 1 — DOS (HP-perovskite), 2 — the shape of DOS (Pb) curves in 3D HP crystal, 3 — DOS (Au) — schematically, not to scale.

along the energy axis) extends to the upper boundary of the gold state spectrum, the second integral (downward along the energy axis) extends to $\varepsilon_{\text{gold}}^{(0)}$, the third integral extends to the lower boundary of the gold level spectrum. This third integral below $\varepsilon_{\text{gold}}^{(0)}$ shall include another overlap integral V_{dd} and another (smaller) mean distance between levels. Change of the form of integrals for $E < \varepsilon_{\text{gold}}^{(0)}$ is quite evident.

By substituting the interface elements of \hat{Q} operators of gold and perovskite in (39) and assuming $\mathbf{k}_z = 0$, we obtain the dispersive relation needed to calculate DOS

$$(\xi_0 \xi_1 - V_{02}^2 + U_1 V_{02}) \xi_{\text{gold}} - U_1 (\xi_0 \xi_1 - V_{02}^2) - U U_2 (V_{02} + \xi_1) - 4V_{\text{dd}} S_x S_y L (\xi_0 \xi_1 - V_{02}^2 + U_1 V_{02}) = 0. \quad (41)$$

Nominators of $\hat{\Pi}$ elements, sum of which is used to calculate the density of states, are calculated according to the same scheme as for \hat{G} , \hat{Q} and are not given here.

The calculated density of states is given in Figure 3.

It can be seen from it and (41) that the „perovskite“ part of \hat{Q} operator, that had no bands and reduced to individual levels, is transformed again in a quite broad band due to the interaction with gold. The same oscillations as on DOS of gold are further visible on the DOS curves, which results from the multiplicity of considered gold levels, however, their amplitude is much lower than that in Figure 5. The DOS curves are narrower than the initial ones that refer to the 3D material, as must be the case when dimension reduces. Extension of the amplitudes of DOS curves into the high energy region with respect to the initial VBM boundary is most substantial.

Extension of the DOS curves results from repulsion of the Pb level from dense gold levels with $E < \varepsilon_{\text{gold}}^{(0)}$, while $6s(\text{Pb})$ and $\varepsilon_{\text{gold}}^{(0)}$ levels are very close to each other. As shown in equation (7), the overlap integral sign is inessential. From that (7), it follows that the width of the formed band with a small overlap integral may be estimated as

$8(8U')^2/(\varepsilon_{6s} - \varepsilon_{\text{gold}}^{(0)})$, which can reach units of V, despite the smallness of U' . The Fermi level shown in Figure 5 above for a bulk gold crystal is kept unchanged compared with $\varepsilon_{\text{gold}}^{(0)}$. It can be seen that the upper edge of the interface states is above ε_F . This means that electrons may be transferred from the metal to the perovskite interface states, though it is limited by a low DOS of interface states compared with that in the „electron sea“ of the metal.

Proximity of $\varepsilon_{\text{gold}}^{(0)}$ to $6s(\text{Pb})$ level seems almost accidental, however, the same effect can also give the gold level at $E > \varepsilon_{\text{gold}}^{(0)}$, which is a little lower in energy than $6s(\text{Pb})$, but closer to $6s(\text{Pb})$ than the next upper level. It is clear that, in the assembly of almost identical interface cells, this is wrong for a significant part of cells, upper boundaries of which „don't reach“ ε_F , but the described mechanism is valid for some cells.

6. Conclusion

Dispersive dependences of electron modes at the hybrid (MA)PbI₃perovskite interface with one of the most effective electrode materials — gold, and the density of interface surface states are discussed. Gold was believed to form with HP a crystallographically perfect interface characterized by (3HP)×(4Au) superlattice. It is too large for *ab-initio* or DFT calculations and there is no periodicity across the interface therefore a stationary Green's operator method in site representation was chosen for the analysis. Input data about 3D lattices of perovskite, gold and interaction between these components were derived from the DFT methods and known calculations. Extension of the upper band $6s$ of Pb, which is VBM in the bulk perovskite, to a level higher than the Fermi energy of gold — appearance of metal-induced states in a semiconductor is the main outcome. Thus, the perovskite interface states may be filled with electrons. Combination of this mechanism with intense electromigration of halogen ions within perovskite, their impact on the temperature dependences of current-voltage curves of the Au/HP/metal systems and resistive switching mechanism will be discussed in a further work.

Conflict of interest

The author declares that he has no conflict of interest.

References

- [1] F. Pan, S. Gao, C. Chen, C. Song. Mater. Sci. Eng. R Rep. **83**, 1–59 (2014).
- [2] A.N. Mikhaylov, E.G. Gryaznov, A.I. Belov, D.S. Korablev, A.N. Sharapov, D.V. Guseinov, D.I. Tetelbaum, S.V. Tikhov, N.V. Malekhonova, A.I. Bobrov, D.A. Pavlov, S.A. Gerasimova, V.B. Kazantsev, N.V. Agudov, A.A. Dubkov, C.M.M. Rosário, N.A. Sobolev, B. Spagnolo. Phys. Status Solidi C **13**, 10–12, 870–881 (2016).
- [3] F. Sunny, S.K. Balakrishnan, N. Kalarikkal. ChemNanoMat **10**, 3, e202300484 (2024).

- [4] P. Schulz, D. Cahen, A. Kahn. *Chem. Rev.* **119**, 5, 3349–3417 (2019). doi: 10.1021/acs.chemrev.8b00558.
- [5] Q. Li, Z. Wang, J. Ma, M. Han, P. Gao, M. Cai, Y. Zhang, Y. Song, S. Peng. *Nano Res.* **17**, 5, 3950–3981 (2024).
- [6] N.I. Alekseev, A.N. Alyoshin. *FTT* **66**, 377 (2024). (in Russian).
- [7] N.N. Shlenskaya, N.A. Belich, M. Grätzel, E.A. Goodilin, A.B. Tarasov. *J. Mater. Chem. A* **6**, 4, 1780–1786 (2018).
- [8] Z. Lai, Y. Zhang, Y. Meng, B. Xiuming. *Small Methods* **7**, 7, 2201567 (2023).
- [9] K. Pydzinska-Białek, G. Nowaczyk, M. Ziółek. *Chem. Mater.* **34**, 14, 6355–6366 (2022).
- [10] S.Yu. Davydov, A.A. Lebedev, O.V. Posrednik. *Fizika poverhnosti i granits rjazdela. Izd-vo SPbGETU „LETI“, SPb* (2013). (2005). p. 66. (in Russian).
- [11] S.Yu. Davydov. *Teoriya adsorbtsii: metod modelnykh gamiltonianov. Izd-vo SPbGETU „LETI“, SPb* (2013). p. 235. (in Russian).
- [12] S.Y. Davydov. *Semiconductors* **45**, 8, 1070–1076 (2011).
- [13] S.Yu. Davydov, A.A. Lebedev, *Nauchno-tekhnikeskij vestnik informatsionnykh tekhnologij, mekhaniki i optiki*, **24**, (2), 665–667 (2024). (in Russian).
- [14] T. Umebayashi, K. Asai, T. Kondo, A. Nakao. *Phys. Rev. B* **67**, 15, 155405 (2003).
- [15] M.H. Du. *J. Mater. Chem. A* **2**, 24, 9091–9098 (2014).
- [16] R. Roseri, F. Antonangeli, U.M. Grassano. *Surf. Sci.* **37**, 689–699 (1973).
- [17] N.E. Christensen, B.O. Seraphin. *Phys. Rev. B* **4**, 10, 3321–3344 (1971).
- [18] J. Tersoff. *Phys. Rev. Lett.* **52**, 6, 465 (1984).
- [19] V. Heine. *Phys. Rev.* **138**, 6A, A1689–96 (1965).

Translated by E.Iinskaya